



Using composite chitosan-graphene oxide to eliminate reactive blue 19 from water solutions: the study of adsorption kinetics and reaction thermodynamics

Masoumeh Beik Mohamadi^{a,b}, Hamide Ejazi^c, Fateme Azadbakht^{d,*}

^aDepartment of Environmental Health Engineering, Faculty of Public Health, Semnan University of Medical Sciences, Semnan, Iran, email: masomebeikmohamadi@yahoo.com

^bDepartment of Environmental Health Engineering, Faculty of Public Health, Tehran University of Medical Sciences, Tehran, Iran

^cStudent Research Committee, Department of Environmental Health Engineering, Faculty of Public Health, Semnan University of Medical Sciences, Semnan, Iran, email: hamide.ejazi@yahoo.com

^dDepartment of Environmental Health Engineering, Faculty of Public Health, Iran University of Medical Sciences, Tehran, Iran, email: fatemeh.azaddakht66@gmail.com

Received 11 June 2018; Accepted 18 January 2019

ABSTRACT

Textile wastewater constitutes a major environmental pollutant. Therefore, eliminating dye from textile wastewater is a main challenge for industrial wastewater treatment plants. Reactive blue 19, which is a common dye used in textile, is resistant to degradation, with stakeholders facing many difficulties in its elimination from water solutions. The current study aimed to examine the effect of composite chitosan-graphene oxide on eliminating reactive blue 19 from water solutions. The study also investigated the kinetics of the related reactions. This empirical study was conducted in a laboratory setting. Graphene oxide was synthesized from graphite powder using modified Hummer's method. It was then doped by chitosan powder and the produced composite synthesized chitosan-graphene oxide was utilized to eliminate reactive blue 19 from water solutions. The effects of initial dye concentration (20, 40, 50, and 60 mg/l), nanocomposite dose (0.1, 0.3, 0.5, 0.7, 1, and 1.5 g/l), pH (4, 7, and 9), and exposure time (10, 20, 30, 40, 60, 90, and 120 min) were studied. The empirical data of adsorption equilibrium were compared with Langmuir adsorption isotherm. The percentages of eliminated dye were analyzed using Perzi. The findings showed that 99% of reactive blue 19 is eliminated from water solutions in optimal conditions (pH = 4, exposure time = 60 min, adsorption dose = 1 g/l, and dye concentration 20 mg/l). It was also discovered that the elimination pattern followed Langmuir isotherm and second-order kinetic model. The results of the present study showed that with the rise of contact time and adsorbent dosage and the decline of reactive blue 19 concentrations, removal efficiency tends to increase. pH = 4, time = 60 min, adsorbent dose = 1 g/l and concentration 20 mg/l were obtained as optimum conditions. Under optimum condition (pH = 4, time = 60 min, adsorbent dose = 1 g/l and concentration 20 mg/l) the highest efficiency of in reactive blue 19 removal is 99%. The adsorption isotherm showed that absorption process correlates well with Langmuir adsorption isotherm ($R^2 > 0.98$). Reaction kinetics complies with Pseudo-second order model with correlation coefficient of ($R^2 = 0.92$). The results showed that synthesized composite chitosan-graphene oxide has the capability of effective elimination of reactive blue 19 from water solutions. Thus, it can be exploited as an effective and efficient adsorbent to treat water solutions and eliminate dye.

Keywords: Reactive blue 19; Chitosan/graphene oxide; Adsorption; Isotherm; Kinetics

* Corresponding author.

1. Introduction

Rapid growth of textile industry has resulted in the widespread contamination of water by synthetic dyes, which are commonly used in industries such as textile, leather, cosmetics, publishing, food, paper production, plastics, and pigment production [1]. Discharging dye compounds in recipient waters has enhanced the biochemical oxygen demand (BOD) of water. Furthermore, dye compounds prevent appropriate light radiation to water, hence decreasing the possibility of photosynthesis and the amount of oxygen dissolved in water. Thus, they hurt the environment and cause death among aquatic creatures [2]. Over 700 tons of dyes are produced annually. In terms of structure, they are classified into various groups such as azo, anthraquinone, and phthalocyanine. Additionally, with regard to their application, dyes are categorized as reactive, acidic, crude, direct, disperse, etc. Reactive dyes, which are water soluble and anionic, are commonly used in dyeing. They have somewhat replaced direct and azo dyes. The widespread use of reactive dyes can be attributed to their ease of use, suitable stability during washing, and low energy consumption. However, they cause many environmental problems; the most serious concern is the danger of their wastewater because of the stability and resistance of such dyes against chemical factors [3]. To date, various strategies, including adsorption, chemical reduction, decomposition, coagulation, biological purification, ozonization, reverse osmosis, ion exchange, and membrane processes, have been used to eliminate dyes from wastewater [4,5]. It has been demonstrated that all these methods are efficient, but adsorption techniques have been considered as an excellent method for effective removal of different types of pollutants. These techniques are effective because of their simple and easy operation, easy application, low costs, high efficiency, and eco-friendly nature [6].

The most commonly used process in this regard is adsorption because of its low cost, high efficiency, simplicity, and non-sensitivity to toxic substances [7]. Recently, graphene has gleaned a lot of attention among researchers due to its unique electronic features and wide specific surface area. It is a good candidate for combination with zinc oxide. It is also known as a superb adsorbent of organic compounds and promotes the adsorption of dye pollutants [8–10]. Chitosan is a distilled chitin derivative which is biodegradable as a cationic polymer. This biopolymer has been used in water and wastewater treatment for three decades. It has an extraordinary capability in coagulation and flocculation of suspended and colloidal particles. It can also be used in the absorption of soluble oil and grease as well as chilled heavy metals. Chitosan can properly replace aluminum salts and polyelectrolyte kinetics in water and wastewater treatment. The efficiency of chitosan in coagulation and flocculation of suspended and colloidal particles and adsorption of soluble ions improves by solving it in acid solution or distilling it in various states. Using chitosan to treat water and wastewater has a number of advantages: reduction in the harmful health effects of the remaining aluminum and synthetic polymers, production of biodegradable sludge, decline of sludge volume, isolation of dissolved metal ions and heavy metals, slight need for pH and alkali regulating chemicals, reduction of soluble ions in water and wastewater, reuse of marine debris, etc [11].

Among different types of adsorbents, graphene and graphene oxide are much better than other types of carbon-based adsorbents (e.g. active carbon and carbon nanotube) because they have a larger adsorbent surface [12]. Graphene is a non-polar, hydrophobic, and insoluble adsorbent and hardly dissolves due to strong covalent bonds in the solvent. Therefore, it can prevent the adsorption of organic compounds and metal ions [13]. Graphene oxide is produced as a result of graphite oxidation and its layering in water or other solvents. It is covered with apophytic, hydroxyl, and carboxyl groups [14,15]. Chitosan, which is an adsorbent with strong functional groups, forms covalent bond with graphene oxide, hence increasing the degree of adsorption by graphene oxide [6,16,17].

Since it contains valuable functional groups in its structure, chitosan can form covalent bonds with graphene oxide, which is accomplished via oxidation and resuscitation reactions [12]. Thus, in order to enhance the adsorption process, the current study aimed at finding the effect of synthesized nanocomposite chitosan-graphene oxide [13,14] on eliminating reactive blue 19, as a representative of dye organic pollutant.

2. Materials and method

2.1. Chemicals and equipment

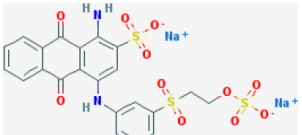
The materials used in this study encompass chitosan ($C_8H_{13}NO_5$), potassium permanganate ($KMnO_4$), sulfuric acid (H_2SO_4), hydrochloric acid (HCl), glutaraldehyde ($C_5H_8O_2$), sodium hydroxide (NaOH), ethanol (C_2H_5OH), hydrogen peroxide (H_2O_2), and methanol (CH_3OH). All these materials were purchased from Merck of Germany. The characteristics and chemical structure of the used dye are presented in Table 1 [15].

Ion-free water was used to prepare all test solutions. To regulate pH, 0.1 molar chloridric acid and sodium hydroxide as well as a pH meter (HACH-Ha-USA) were utilized. A 6,000 rpm centrifuge was used for 15 min to separate the adsorbent from the solution after the reaction. Finally, a spectrophotometer (JENWAY6053) was exploited to assess the concentration of the remaining dye after the reaction.

2.2. Composite synthesis of chitosan-graphene oxide (CGO)

Graphene oxide was synthesized from graphite powder using modified Hummer's method [16]. More

Table 1
Characteristics and chemical structure of reactive blue 19

Chemical formula	$C_{22}H_{16}N_2Na_2O_{11}S_3$
Brand name	Remazol Brilliant Blue R
Category	Azo
Molecular weight	626.533 g/mol
Adsorption wavelength	592 nm
Molecular structure	

specifically, 1 g of graphite powder and 25 ml of sulfuric acid were mixed in the reaction vessel, with the temperature remaining at $0^{\circ}\text{C} \pm 2^{\circ}\text{C}$ by the use of an ice water bath. Then, 3 g of potassium permanganate were slowly added to the vessel, followed by heating the mixture in a magnetic stirrer under the temperature of $35^{\circ}\text{C} \pm 2^{\circ}\text{C}$ for 2 h. During this time, the mixture was slowly stirred. Subsequently, some hydrogen peroxide (5 ml) was added until no gas bubble was observed. Graphene oxide powder was then obtained through drying the mixture under the temperature of 65°C for 12 h. The mixture was subsequently exposed to ultrasonic waves with a frequency range of 50–60 Hz using an ultrasonic bath, a stage that lasted for 3 h at room temperature. This yielded graphene oxide powder [17]. The powder was then added to a vessel containing 23 ml of 1% acetic acid, followed by exposing the mixture to ultrasonic waves for 33 min in the room temperature. After that, 0.5 g of chitosan was added to the vessel and the mixture was further exposed to ultrasonic waves for 1 h. After 12 h, 3% sodium hydroxide was gradually added to the mixture to enhance the pH to 9–10. After 24 h, the formed particles [18] were washed several times using distilled water, reducing the pH to 7. The bids were then transferred to a 253 ml flask, where 33 ml of methanol and 1.5 ml of glutaraldehyde were added to them. The mixture was stirred for 5 h at room temperature using a shaker. At the end, the bids were filtered and washed several times by the use of ethanol and distilled water [13,17,19]. The obtained powder was nanocomposite chitosan-graphene oxide.

2.3. Assessing the features of the synthesized composite chitosan-graphene oxide (CGO)

X-ray diffusion (XRD) was used to assess the structure of the synthesized composite. FTIR spectrum was further exploited to determine functional groups at the surface of nanoparticles. Finally, scanning electron microscope (SEM) was utilized to examine the morphology of composite chitosan-graphene oxide. All analyses were conducted in Tarbiat Modares University.

2.4. Procedure

This applied study was an experimental test in a laboratory setting. First, a stock solution of reactive blue 19 was produced, followed by preparing different concentrations of it. The pH of the samples was regulated using 0.1 molar hydrochloric acid and sodium hydroxide. Then, in order to perform the tests, a particular amount of synthesized adsorbent was added to an Erlenmeyer flask containing 100 cc of the sample with a specific concentration. The mixture was then stirred using a 200 rpm shaker. After particular intervals, a proportion of the mixture inside the Erlenmeyer was taken and centrifuged. Then, the adsorption capacity of the remaining dye was gauged at 592 nm. The measurement was conducted using spectrophotometer [20]. Finally, the amount of remaining dye was assessed via line equation. To optimize factors that might affect the adsorption process, a parameter was held constant and the influence of other parameters was gauged. The tests were repeated twice. The following equations were used to calculate the amount of adsorbed dye and the percentage of dye eliminated by chitosan graphene oxide:

$$R = \frac{(C_0 - C_e)}{C_0} \times 100 \quad (1)$$

$$q_t = \frac{(C_0 - C_e)v}{M} \quad (2)$$

In these equations, R is the percentage of eliminated dye, C_0 is the initial dye concentration (mg/l), C_e is the concentration of the remaining dye in the solution (mg/l), q_t is the amount of adsorbed dye during time (mg/g), q_e is the amount of adsorbed dye in the equilibrium status (mg/g), V is the solution volume (l), and M is the adsorbent dose (g). The present study focused on the impact of the initial dye concentration (20, 40, 50, and 60 mg/l), pH (4, 7, 9), adsorbent dose (0.1, 0.3, 0.5, 0.7, 1, and 1.5 g/l), and exposure time (10, 20, 30, 40, 60, 90, and 120 min) were examined [9,15,21]. To come up with the optimal condition, the impacts of adsorbent dosage (0.1, 0.3, 0.5, 0.7, and 1 g/l), pH (2, 7, and 9), concentration (20, 40, 50, and 60 mg/l), and exposure time (10, 20, 30, 40, 60, 90, and 120 min) were measured.

3. Results

3.1. Features of the synthesized CGO

3.1.1. SEM analysis

SEM was used to assess the surface features and morphology of graphene oxide and composite chitosan-graphene oxide (Fig. 1). The recorded images show that graphene oxide has a laminated and wrinkled surface, while composite chitosan-graphene oxide has appropriate porosity and a relatively homogeneous distribution.

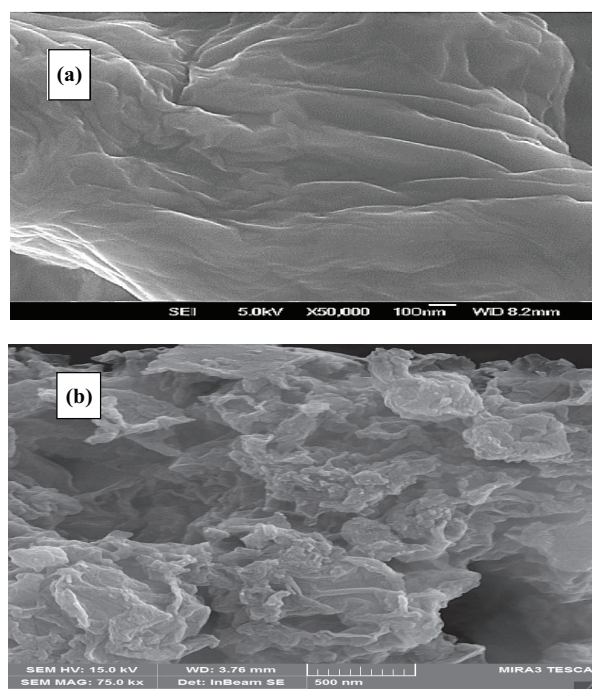


Fig. 1. SEM image of (a) graphene oxide (GO) and (b) chitosan-graphene oxide (CGO).

3.1.2. XRD analysis

Moreover, XRD was used to assess the structure of the synthesized adsorbent. Fig. 2(a) represents XRD analysis of graphite and grapheme and graphene oxide, and Fig. 2(b) represents XRD analysis of composite chitosan graphene oxide by the use of Cu K α within the angular range of $2\theta = 2-100$. XRD analysis yielded a peak at $2\theta = 20.3$, which is attributed to the irregular structure of chitosan. Another peak was observed at $2\theta = 21.2$, which can be attributed to chitosan-graphene oxide.

3.1.3. FTIR analysis

FTIR spectrum was used to determine functional groups at the adsorbent surface. The results of chitosan graphene oxide FTIR are presented in Fig. 3. In the FTIR curve of graphene oxide, the three peaks (1,732, 1574, and 1211.82 cm^{-1}) are respectively attributed to C=O in the carboxylic group, C=C bond, and C-O. All three peaks have changed in the FTIR analysis of chitosan-graphene oxide, which can be attributed to the hydrogen bonding between chitosan and graphene oxide. Additionally, in the FTIR curve of chitosan, the 1,659 peak is related to C=O in -NHCO-. On the other hand, in the FTIR curve of composite chitosan-graphene oxide, the peaks within the range of 3,300–3,400 cm^{-1} are related to the OH group, and the peak at 1,634 cm^{-1} has to do with the C=C bond.

3.2. The effect of solution pH

The effect of three different pHs (4, 7, and 9) on dye removal efficiency was investigated while other variables remained constant (initial dye concentration: 20 mg/l ,

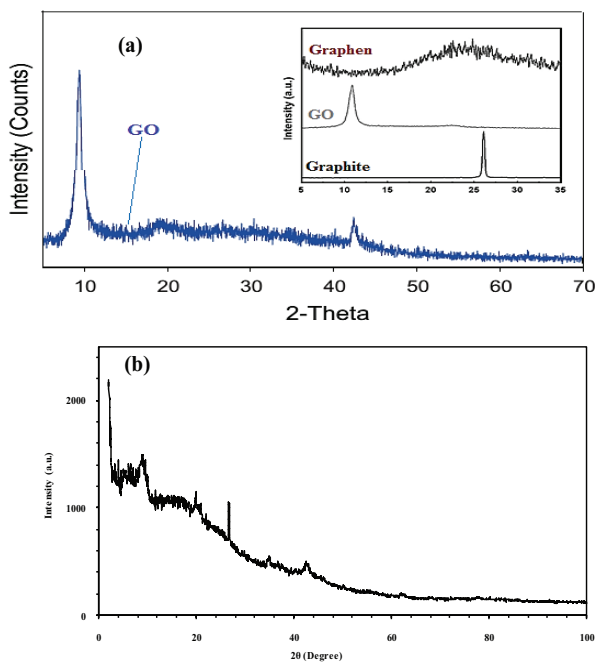


Fig. 2. XRD analysis of (a) graphene, graphite and grapheme oxide and (b) composite chitosan graphene oxide.

adsorbent dose: 1 g/l , and exposure time 10–120 min). It was discovered that increasing pH would reduce the amount of removal dye. The highest dye elimination efficiency (99.1%) occurred when the pH was 4, whereas the lowest one (68.35%) was recorded when the pH was 9 (Fig. 4). Thus, the highest amount of dye elimination was registered at the pH of 4.

3.3. The effect of exposure time

The effect of exposure time was investigated by changing the exposure time from 10 to 120 min while the other variables remained constant (the initial dye concentration: 20 mg/l , adsorbent dose: 1 g/l , and pH: 4) (Fig. 5). Therefore, increasing the exposure time from 10 to 60 min improved the elimination efficiency from 5% to 98.85%. The maximum amount of adsorption occurred during the first 60 min. Thus, the optimal time period for having the highest elimination efficiency is 60 min. increasing the exposure time from 60 to 120 min did not significantly change the proportion of adsorption.

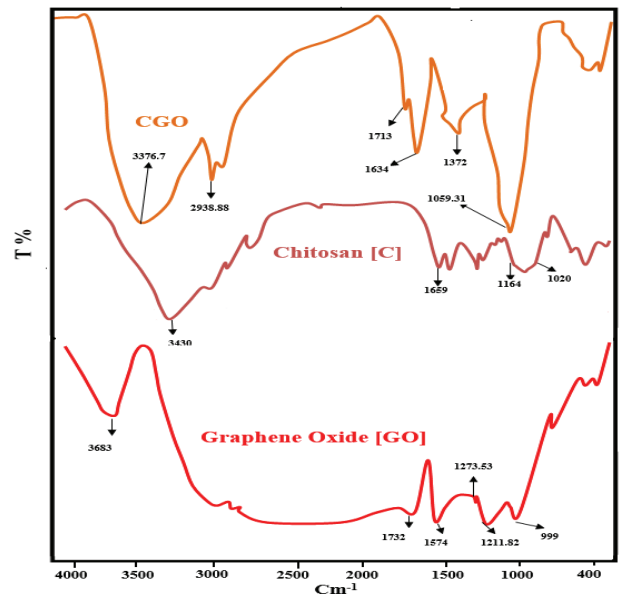


Fig.3. FTIR spectrum of chitosan, graphene oxide, and composite chitosan graphene oxide.

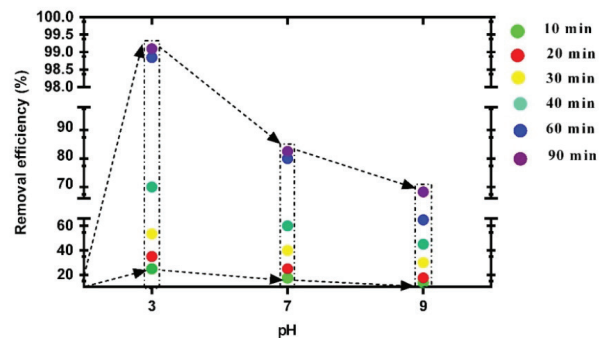


Fig. 4. Effect of pH on the efficiency of eliminating reactive blue 19.

3.4. The effect of initial dye concentration

The effect of dye concentration was investigated using four different concentrations (20, 40, 50, and 60 mg/l) while adsorbent dose and pH remained constant at 1 g/l and 4, respectively. The results indicated that increasing dye concentration from 20 to 60 mg/l would yield lower elimination efficiency (Fig. 6). As a result, the highest dye elimination efficiency (99%) was recorded when the initial dye concentration was 20 mg/l.

3.5. The effect of chitosan graphene oxide dose

The effect of various doses of chitosan graphene oxide (0.1 through 1/2 mg/l) on dye removal efficiency was investigated while pH was 4 (Fig. 7). The results revealed that increasing the adsorbent dose would lead to higher elimination efficiency. Thus, increasing the adsorbent dose from

0.1 to 1.2 g/l while dye concentration was 20 mg/l improved the efficiency of dye removal.

3.6. Adsorption isotherm of reactive blue 19 using chitosan graphene oxide

Adsorption isotherm consists of some equations used to explicate the adsorbate equilibrium between solid and fluid phases. In the current study, Freundlich and Langmuir adsorption isotherms were used to empirically describe the data. Langmuir isotherm has to do with homogeneous adsorbent surfaces with fixed energy, while Freundlich isotherm is based on heterogeneous adsorbent surfaces with non-uniform distribution. Table 2 displays the isotherm equations and formulas. Figs. 8 and 9 show the Freundlich and Langmuir adsorption isotherm for adsorbing reactive blue 19.

As major parameters in Langmuir isotherm, RL indicates the adsorbent’s capability to separate pollutants. It is calculated through the following formula:

$$RL = \frac{1}{1 + bC_0} \tag{3}$$

Adsorption is ideal when $0 < RL < 1$, while it is inappropriate when $RL > 1$. If $RL = 1$, adsorption is linear and if $RL = 0$, adsorption is irreversible [22,23]. In Table 3 the results of this study showed that RL was smaller than 1, hence the adsorption of reactive blue 19 by the use of chitosan-graphene oxide was suitable.

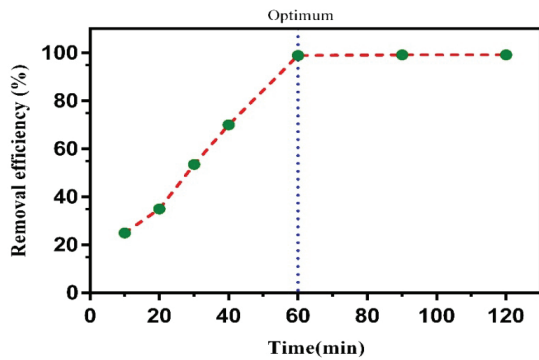


Fig. 5. Effect of time on the efficiency of eliminating reactive blue 19.

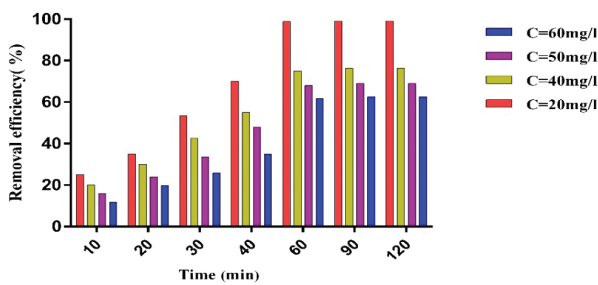


Fig. 6. Effect of dye concentration on the efficiency of eliminating reactive blue 19.

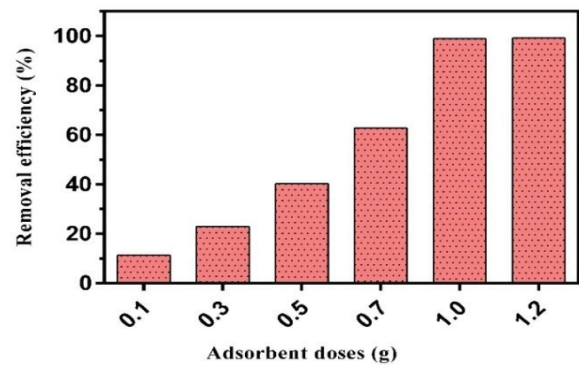


Fig. 7. Effect of chitosan graphene oxide dose on the efficiency of eliminating reactive blue 19.

Table 2
Freundlich and Langmuir isotherm equations

Isotherm	Linear equation	Diagram	Parameter
Freundlich	$\ln q_e = \ln K_f + (n^{-1}) \ln C_e$	$\ln q_e$ vs. $\ln C_e$	$K_f = \exp(\text{intercept})$ $n = (\text{slope})^{-1}$
Langmuir	$\frac{C_e}{q_e} = (1/k_l q_m) + (\frac{C_e}{q_m})$	$1/q_e$ vs. $1/C_e$	$q_m = (\text{intercept})^{-1}$ $K_l = \text{intercept/slope}$

3.7. Adsorption kinetics of reactive blue 19 using chitosan-graphene oxide

First- and second-degree kinetic models were used to assess the performance of the adsorbent and the adsorption mechanism. In the current study, the passage of time enhanced the proportion of adsorbed reactive blue 19, with the highest adsorption percentage (98.85%) being recorded after 60 min. After this time, a negligible increase was observed in the adsorption rate. Table 4 illustrates the kinetic and equilibrium models of reactive blue 19 adsorption. In this table, q_t and q_e respectively are the amount of adsorbed

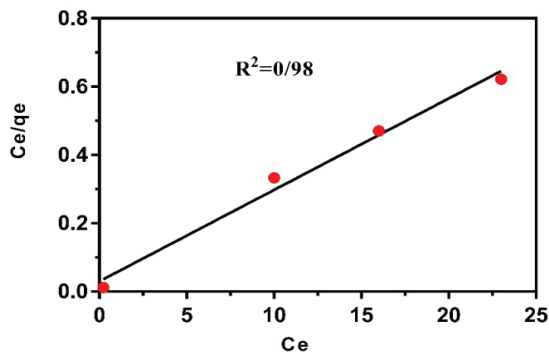


Fig. 8. Langmuir adsorption isotherm for adsorbing reactive blue 19.

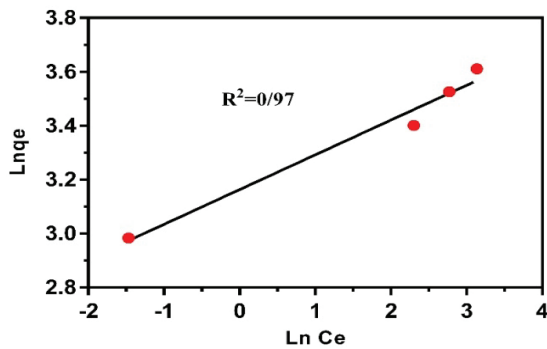


Fig. 9. Freundlich adsorption isotherm for adsorbing reactive blue 19.

Table 3
Parameters of reactive blue 19 adsorption isotherms by the use of chitosan-graphene oxide

Isotherm	Parameter	Adsorption
Freundlich	R^2	0.97
	$1/n$	0.12
	K_f	23.65
Langmuir	R^2	0.98
	RL	0.63
	q_m	40

dye for each gram of the adsorbent during time (t) and in the equilibrium status (mg/g). K_1 is the first-order kinetic constant (1/min), while K_2 is the second-order kinetic constant (1/min). Computational adsorption capacity (q_{cal}) is determined by drawing $\ln(q_e - q_t)$ diagram against t . Figs. 10 and 11 depict the first- and second-order kinetic models for adsorbing reactive blue 19 by chitosan-graphene oxide. It is observed that the adsorption process has majorly followed the second-order kinetic model.

3.8. Adsorption thermodynamics

The results of examining the adsorption thermodynamics are presented in Table 5. It is observed that the values of ΔH° and ΔS° for reactive blue are -20.89 and 0.1 , respectively. The ΔG° values in temperatures of 30°C , 20°C , and 50°C are also demonstrated in Table 5.

4. Discussion

4.1. Adsorption characteristics of CGO

4.1.1. SEM analysis

As indicated by the results of SEM (Fig. 1), GO has a flat surface with a sheet-like structure, high thickness, and corrugated edges [22,26]. According to SEM images, when GO is combined with chitosan, the density of the new compound goes up, an indication of the strong bond between chitosan and graphene oxide. Nonetheless, it is hard to blend or cover graphene oxide with a layer of chitosan, while the graphene oxide sheet is clearly observable. This demonstrates that chitosan and graphene oxide have been appropriately connected. Donglin et al. [27] came to the same conclusion.

4.1.2. XRD analysis

Fig. 2 illustrates the XRD analysis of chitosan graphene oxide composite using Cu $K\alpha$ beam in the angular range of $2\theta = 100-2$. In their study, Justin et al. attributed the frequencies of $2\theta = 11$ and $2\theta = 20$ to chitosan [28]. Also, Kumar et al. [21] indicated that the frequency of $2\theta = 21.18$ has to do with chitosan graphene oxide.

Table 4

Kinetic parameters of adsorbing reactive blue 19 by chitosan-graphene oxide

Adsorbate	Kinetic model
First-order model	
0.70	R^2
6.5	$q_{e,cal}$ (mg/g)
0.011	K_1
Second-order model	
0.92	R^2
30	$q_{e,cal}$ (mg/g)
0.0006	K_2
$q_{e,exp} = 37$	

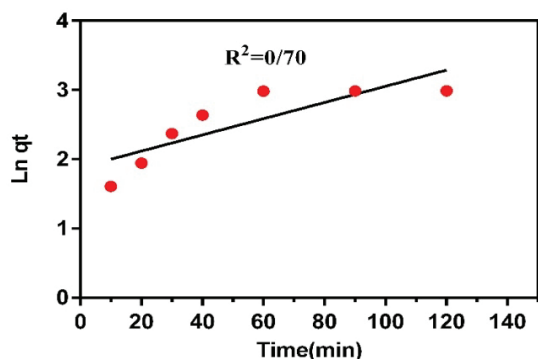


Fig. 10. First-order kinetic model for adsorbing reactive blue 19 by chitosan-graphene oxide.

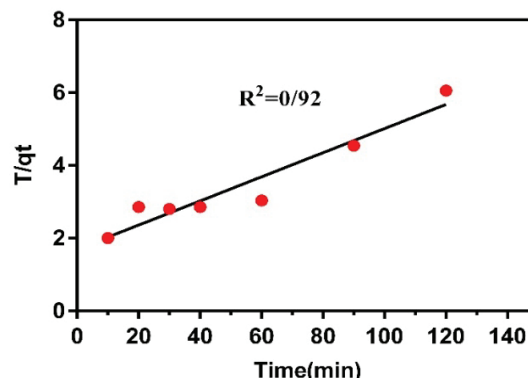


Fig. 11. Second-order kinetic model for adsorbing reactive blue 19 by chitosan-graphene oxide.

Table 5

Adsorption thermodynamic parameters for adsorbing reactive blue 19 by chitosan-graphene oxide

Adsorbate	T (K°)	$\ln K_c$	ΔG° (kJ/mol)	ΔH° (kJ/mol)	ΔS° (kJ/mol.K)
Reactive blue	293	4.56	-11.11	-20.89	0.1
	303	4.88	-12.20		
	323	5.58	-14.99		

4.1.3. FTIR analysis

The results of FTIR analysis of chitosan, graphene oxide, and chitosan graphene oxide composite are displayed in Fig. 3. In Justin et al.'s [28] study, the frequencies of 1,727 and 1,628 cm^{-1} were respectively attributed to C=O and C=C in graphene oxide. Further, the frequencies of 1,530 and 1,540 cm^{-1} were attributed to C=O in -NHCO- in chitosan. Their results are in line with the findings of this study [25]. The results of TIR, SEM, and XRD analysis shed light on the chemical structure and mixture of the synthesized adsorbent, i.e. chitosan-graphene oxide. The findings are in agreement with the results of previous studies [16,24,26].

4.2. The effect of solution pH

According to Fig. 4, the results of examining the effect of pH on removal reactive blue 19 showed that increasing solution pH would lead to lower elimination percentage. This can be attributed to the increase in the number of H^+ ions and the reduction of OH^- ions as well as the number of positive ions on the adsorbent surface. The dye that was used in this study will carry negative charge in water solutions, a phenomenon that improves the adsorption efficiency in lower pH. Indeed, in low pH, the activated carbon surface area will have positive charge leading to electrostatic interaction between the adsorbent and the dye. Decreasing pH will result in more areas with positive charge. These areas are more likely to adsorb dye due to the electrostatic gravity [27,28]. Jamshidi et al. [15] who examined the elimination of reactive blue 19 by the use of pomegranate seed powder, came to the same conclusion. They revealed that increasing pH from 3 to 11 would lower dye elimination efficiency.

Ozcan et al. [29] also indicated that increasing pH from 1.5 to 8.5 would decline the efficiency of eliminating reactive blue 19. They recorded the highest elimination percentage when the pH was 1.5.

According to previously conducted studies, the amount of pH_{pzc} for chitosan, graphene oxide, and chitosan graphene oxide composite respectively are 8.9–9 [30–34], 3.9–4.12 [35,36], and 5.45 [37]. The amount of pH_{pzc} observed in this study was 7.21. In pHs that are greater than pH_{pzc} the potential charge is on the negative adsorbent, while in pHs that are smaller than pH_{pzc} it is on the surface of the positive adsorbent. Also, in pHs that are equal to pH_{pzc} the adsorbent has no charge. Thus, in pHs that are smaller than 7.21, electrostatic bond is formed between the adsorbent and the dye because the adsorbent has positive charge. In pHs greater than 7.21, the adsorbent and the dye both have negative charge, which causes electrostatic repulsion between them, hence the amount of adsorbed dye reduces. In the study conducted by Dizge et al., [38] the pH_{zpc} for fly ash to eliminate blue reactive 19 was found to be 7.0.

4.3. The effect of exposure time

Exposure time is another factor that may influence dye elimination. According to Fig. 5, higher elimination efficiency was recorded in longer exposure times. However, no significant increase was observed in dye elimination after 60 min of exposure. In fact, at the beginning of adsorption, dye molecules are rapidly adsorbed by the surface of the adsorbent. Nonetheless, in the course of time, the adsorption speed dwindles because of the relative electrostatic repulsive forces of the adsorbed negative charges at the surface of the adsorbent, negative charges in the fluid mass, and the pollutant

emission rate inside the porosities [32,36]. Ghaneian et al. [37] reported the same findings while examining the elimination of reactive blue 19 by the use of straw powder.

4.4. The effect of initial dye concentration

Based on Fig. 6, increasing the initial dye concentration would result in lower efficiency of reactive blue 19 elimination. Given that the adsorption areas are fixed in particular amount of adsorbent, it is plausible to speculate that increasing initial dye concentration will lower dye elimination efficiency. Furthermore, the declining ratio of remaining dye to the initial dye concentration (which is observed after increasing dye concentration) can be attributed to the driving force that is created as a result of increasing initial concentration. This force creates repulsion between dye molecules, reducing the percentage of adsorbed dye [30,38–40]. Mousavi et al. [41] studied the adsorption isotherm and kinetics of reactive blue 19 from water solutions using multiwall carbon nanotubes. They demonstrated that enhancing the initial dye concentration results in lower adsorption efficiency. Some other studies have come to similar conclusions [37,42,43].

4.5. The effect of chitosan-graphene oxide dose

The influence of the amount of adsorbent is typically examined while studying the adsorption process. According to the obtained results, increasing the dose of adsorbent from 0.1 to 1.5 mg/l would enhance dye elimination efficiency. The same results were reported by Ghaneian et al. [20] who studied elimination of reactive blue 19 using squid bone powder. They believed that this higher elimination efficiency can be attributed to more surface area of the adsorbent and higher number of adsorption points which are the result of increasing the adsorbent dose. Many other researchers have come to the same conclusion [41,44,45].

4.6. Adsorption kinetics and isotherm of reactive blue 19 using chitosan-graphene oxide

The results of Langmuir and Freundlich isotherms are illustrated in Figs. 8 and 9. The regression coefficient of the adsorbent indicates that the adsorption of reactive blue 19 follows Langmuir isotherm. Therefore, single-layer surface adsorption takes place in particular homogeneous places. Additionally, in this study, the RL value was between 0 and 1, demonstrating the suitability of adsorption [41]. First- and second-order kinetic diagrams were drawn to assess the speed and degree of dye elimination [45]. The results showed that reactive blue 19 elimination by the use of chitosan-graphene oxide follows the second-degree kinetic model with a correlation coefficient of 0.92 and the adsorption mechanism is chemical.

4.7. Adsorption thermodynamics of reactive blue 19 using chitosan-graphene oxide

Examining the adsorption thermodynamics (Table 5) showed that the value of ΔH° was negative, meaning that the adsorption process was exothermic. Furthermore, a negative value was obtained for ΔS° , which indicates irregular

reduction in the equilibrium of solid and liquid phases as a result of heightened temperature during the adsorption process. Moreover, a negative value was registered for ΔG° , demonstrating the spontaneity of reactive blue 19 adsorption by the adsorbent [41]. Additionally, the increase of ΔG° value in higher temperatures shows that adsorption capacity goes up in higher temperatures.

5. Conclusion

The results of this study show that synthesized chitosan-graphene oxide can effectively eliminate reactive blue 19 from water solutions. The highest elimination efficiency was recorded in acidic pH after 60 min of exposure. Therefore, synthesized chitosan-graphene oxide can be utilized as a new adsorbent to eliminate environmental pollutants that are resistant to degradation. Perhaps, the major advantages of this adsorbent over the other ones are the need for smaller adsorbent doses and the higher elimination efficiency in shorter time periods.

Acknowledgements

This paper is based on a university student proposal approved by Semnan University of Medical Sciences and Health Services (proposal number: 1054). We should express our sincere gratitude to the university's research department and the research committee of Aradan School of Public Health and Paramedical Sciences. We are also indebted to our colleagues at the laboratory and the Department of Environmental Health Engineering. It would have been hard to complete this project without their kind help.

References

- [1] M. Li, J.-T. Li, H.-W. Sun, Sonochemical decolorization of acid black 210 in the presence of exfoliated graphite, *Ultrason. Sonochem.*, 15 (2008) 37–42.
- [2] M. Ghodsian, B. Ayati, H. Ganjidoost, Determination of optimum amounts of effective parameters in reactive dyes removal using photocatalytic reactions by immobilized TiO_2 nano particles on concrete surface., *Water. Wastewater.*, 24 (2013) 45–53.
- [3] A. Almasi, Y. Yousefi, M. Soltanian, A. Hashemian, A.R. Mousavi, Investigation of efficiency on reactive red 2 dye decolorization by Fenton/ultrasonic process, *Water. Wastewater.*, 26 (2015) 11–21.
- [4] G. Bharath, E. Alhseinat, N. Ponpandian, M. Ali Khan, M. Raza Siddiqui, F. Ahmed, E. H. Alsharaeh, Development of adsorption and electrosorption techniques for removal of organic and inorganic pollutants from wastewater using novel magnetite/porous graphene-based nanocomposites, *Sep. Purif. Technol.*, 188 (2017) 206–218.
- [5] P. Sathishkumar, M. Arulkumar, T. Palvannan, Utilization of agro-industrial waste *Jatropha curcas* pods as an activated carbon for the adsorption of reactive dye Remazol Brilliant Blue R (RBBR), *J. Cleaner. Prod.*, 22 (2012) 67–75.
- [6] R.R. Kalantary, A. Azari, A. Esrafil, K. Yaghmaeian, M. Moradi, K. Sharafi, The survey of Malathion removal using magnetic graphene oxide nanocomposite as a novel adsorbent: thermodynamics, isotherms, and kinetic study, *Desal. Wat. Treat.*, 57 (2016) 28460–28473.
- [7] M.H. Karaoglu, M.D., M. Alkan, Kinetic analysis of reactive blue 221 adsorption on kaolinite, *Desalination*, 256 (2010) 154–165.
- [8] M. Wang, L. Cai, Q. Jin, H. Zhang, S. Fang, X. Qu, Q. Zhang, One-pot composite synthesis of three-dimensional graphene

- oxide/poly (vinyl alcohol)/TiO₂ microspheres for organic dye removal, *Sep. Purif. Technol.*, 172 (2017) 217–226.
- [9] A. Azari, M. Salari, M.H. Dehghani, M. Alimohammadi, H. Ghaffari, K. Sharafi, N. Shariatifar, M. Baziar, Efficiency of magnetized graphene oxide nanoparticles in removal of 2, 4 dichlorophenol from aqueous solution, *J. Mazandaran. Univ. Med. Sci.*, 26 (2017) 265–281.
- [10] X. Liu, L. Pan, T. Lv, G. Zhu, T. Lu, Z. Sun, C. Sun, Microwave-assisted synthesis of TiO₂ reduced graphene oxide composites for the photocatalytic reduction of Cr (VI), *RSC. Adv.*, 1 (2011) 1245–1249.
- [11] N. Sheikh, S. Kianfar, Using adsorption isotherm studies to determine crosslinked polymeric adsorbent performance in heavy metals removal from water, *Water. Wastewater.*, 25 (2014) 20–29.
- [12] K. Bustos-Ramírez, A.L. Martínez-Hernández, G. Martínez-Barrera, M. Icaza, VM. Castaño, C. Velasco-Santos, Covalently bonded chitosan on graphene oxide via redox reaction, *Materials (Basel)*, 6 (2013) 911–926.
- [13] P.I.M. Firmino, M.E.R. da Silva, F.J. Cervantes, A.B. dos Santos, Colour removal of dyes from synthetic and real textile wastewaters in one- and two-stage anaerobic systems, *Bioresour. Technol.*, 101 (2010) 7773–7779.
- [14] A. Rezaee, M. Ghaneian, A. Khavanin, S. Hashemian, G. Moussavi, Photochemical oxidation of reactive blue 19 dye (RB19) in textile wastewater by UV/K₂S₂O₈ process, *Iran. J. Environ. Health. Sci. Eng.*, 5 (2008) 95–100.
- [15] M. Dehvari, M.T. Ghaneian, A. Ebrahimi, B. Jamshidi, M. Mootab, Removal of reactive blue 19 dyes from textile wastewater by pomegranate seed powder: isotherm and kinetic studies, *Int. J. Env. Health. Eng.*, 5 (2016) 1–9.
- [16] S. Kumar, J. Koh, Physicochemical and optical properties of chitosan based graphene oxide bionanocomposite, *Int. J. Biol. Macromol.*, 70 (2014) 559–564.
- [17] R. Sitko, B. Zawisza, E. Malicka, Graphene as a new sorbent in analytical chemistry, *TrAC. Trends. Anal. Chem.*, 51 (2013) 33–43.
- [18] L. Fan, C. Luo, M. Sun, H. Qiu, X. Li, Synthesis of magnetic β-cyclodextrin–chitosan/graphene oxide as nano-adsorbent and its application in dye adsorption and removal, *Colloids. Surf., B.*, 103 (2013) 601–607.
- [19] N. Bolong, A. Ismail, MR. Salim, T. Matsuura, A review of the effects of emerging contaminants in wastewater and options for their removal, *Desalination*, 239 (2009) 229–246.
- [20] MT. Ghaneian, M. Momtaz, M. Dehvari, An investigation of the efficacy of Cuttlefish bone powder in the removal of Reactive Blue 19 dye from aqueous solutions: equilibrium and Isotherm studies, *Community. Health. Res.*, 1 (2012) 1–11.
- [21] A. Azari, H. Gharibi, B. Kakavandi, G. Ghanizadeh, A. Javid, A.H. Mahvi, K. Sharafi, T. Khosravia, Magnetic adsorption separation process: an alternative method of mercury extracting from aqueous solution using modified chitosan coated Fe₃O₄ nanocomposites, *J. Chem Technol. Biotechnol.*, 92 (2017) 188–200.
- [22] G.-Q. Wu, X. Zhang, H. Hui, J. Yan, Q.-S. Zhang, J.-L. Wan, Y. Dai, Adsorptive removal of aniline from aqueous solution by oxygen plasma irradiated bamboo based activated carbon, *J. Chem. Eng.*, 185 (2012) 201–210.
- [23] K. Foo, B.H. Hameed, Insights into the modeling of adsorption isotherm systems, *J. Chem. Eng.*, 156 (2010) 2–10.
- [24] D. Han, L. Yan, W. Chen, W. Li, Preparation of chitosan/graphene oxide composite film with enhanced mechanical strength in the wet state, *Carbohydr. Polym.*, 83 (2011) 653–658.
- [25] R. Justin, B. Chen, Characterisation and drug release performance of biodegradable chitosan– graphene oxide nanocomposites, *Carbohydr. Polym.*, 103 (2014) 70–80.
- [26] L. Li, C. Luo, X. Li, H. Duan, X. Wang, Preparation of magnetic ionic liquid/chitosan/graphene oxide composite and application for water treatment, *Int. J. Biol. Macromol.*, 66 (2014) 172–178.
- [27] Y. Hamzeh, Azadeh, S. Izadyar, Removal of reactive Remazol Black B from contaminated water by lignocellulosic waste of canola stalks, *J. Color. Sci. Tech.*, 5 (2011) 77–85.
- [28] P. Janos, H. Buchtova, M. Rýznarová, Sorption of dyes from aqueous solutions onto fly ash, *Water. Res.*, 37 (2003) 4938–4944.
- [29] A. Özcan, Ç. Ömeroğlu, Y. Erdoğan, A.S. Özcan, Modification of bentonite with a cationic surfactant: an adsorption study of textile dye Reactive Blue 19, *J. Hazard. Mater.*, 140 (2007) 173–179.
- [30] X. Wu, H. Hong, X. Liu, W. Guan, L. Meng, Y. Ye, Y. Ma, Graphene-dispersive solid-phase extraction of phthalate acid esters from environmental water, *Sci. Total. Environ.*, 444 (2013) 224–230.
- [31] J. Kang, H. Liu, Y.M. Zheng, J. Qu, JP. Chen, Systematic study of synergistic and antagonistic effects on adsorption of tetracycline and copper onto a chitosan, *J. Colloid. Interface. Sci.*, 344 (2010) 117–125.
- [32] G. Zhao, J. Li, X. Ren, C. Chen, X. Wang, Few-layered graphene oxide nanosheets as superior sorbents for heavy metal ion pollution management, *Environ. Sci. Technol.*, 45 (2011) 10454–10462.
- [33] S.-G. Wang, X.F. Sun, X.W. Liu, W.X. Gong, B.Y. Gao, N. Bao, Chitosan hydrogel beads for fulvic acid adsorption: behaviors and mechanisms, *Chem. Eng. Sci.*, 142 (2008) 239–247.
- [34] W. Cheng, W. Cheng, M. Wang, Z. Yang, Y. Sun, C. Ding, The efficient enrichment of U (VI) by graphene oxide-supported chitosan, *RSC. Adv.*, 4 (2014) 61919–61926.
- [35] N. Dizge, C. Aydinler, E. Demirbas, M. Kobya, S. Kara, Adsorption of reactive dyes from aqueous solutions by fly ash: kinetic and equilibrium studies, *J. Hazard. Mater.*, 150 (2008) 737–746.
- [36] M. Amrollahi, M.T. Ghaneian, M. Dehvari, M. Taghavi, B. Jamshidi, Application of pomegranate seed powder in the removal of Reactive Red 198 dye from aqueous solutions, *J. Health. Sci.*, 4 (2012) 45–56.
- [37] S. Mozafari, M.T. Ghaneian, M. Dehvari, B. Jamshidi, Removal of reactive blue 19 from synthetic textile wastewater with using straw powder, *J. IJUMS*, 23 (2016) 119–131.
- [38] X. Song, X. Cheng, X. Yang, D. Li, R. Linghu, Correlation between the bond dissociation energies and impact sensitivities in nitramine and polynitro benzoate molecules with polynitro alkyl groupings, *J. Hazard. Mater.*, 150 (2008) 317–321.
- [39] M. Entezari, Z.S. Al-Hoseini, N. Ashraf, Fast and efficient removal of Reactive Black 5 from aqueous solution by a combined method of ultrasound and sorption process, *J. Ultrason. Sonochem.*, 15 (2008) 433–437.
- [40] S. Azizian, Kinetic models of sorption: a theoretical analysis, *J. Colloid. Interface Sci.*, 276 (2004) 47–52.
- [41] P. Mosavi, MH. Emam Jome, Investigation of isotherm and kinetics of adsorption of reactive blue 19 from aquatic solutions by multiwalled carbon nanotubes, *J. Shahrekord. Univ. Med. Sci.*, 16 (2014) 72–80.
- [42] H.J. Mansoorian, A.J. Jafari, A.R. Yari, A.H. Mahvi, M. Alizadeh, H. Sahebani, Application of acatiortilis shuck as of low-cost adsorbent to removal of azo dyes reactive red 198 and blue 19 from aqueous solution, *Arch. Hyg Sci.*, 3 (2014) 165–175.
- [43] M. Ghaneian, M. Ehrampoush, M. Dehvari, B. Jamshidi, M. Amrollahi, A survey of the efficacy of cuttle fish bone powder in the removal of reactive red 198 dye from aqueous solution, *Toloo e Behdasht.*, 10 (2011) 127–138.
- [44] M. Dehvari, M.T. Ghaneian, F. Fallah, M. Sahraee, B. Jamshidi, Evaluation of maize tassel powder efficiency in removal of reactive red 198 dye from synthetic textile wastewater., *Commun. Health. Res.*, 1 (2013) 153–165.
- [45] M. Elkady, A.M. Ibrahim, M.A. El-Latif, Assessment of the adsorption kinetics, equilibrium and thermodynamic for the potential removal of reactive red dye using eggshell biocomposite beads, *Desalination*, 278 (2011) 412–423.